

Electronic and Optical Properties of Lead-Free Hybrid Perovskite $\text{CH}_3\text{NH}_3\text{SnI}_3$ from First Principles Calculations

Ibrahim Omer Abdallah^{1,2}, Daniel P Joubert¹, and Mohammed S H Suleiman^{1,3}

¹ The National Institute for Theoretical Physics, School of Physics and Mandelstam Institute for Theoretical Physics, University of the Witwatersrand, Johannesburg, Wits 2050, South Africa.

² Department of Scientific Laboratories, Sudan University of Science and Technology, Khartoum, Sudan.

³ Department of Basic Sciences, Imam Abdulrahman Bin Faisal University, P. O. Box 1982, Dammam, KSA.

E-mail: ibrphysics@gmail.com

Abstract. Organic-inorganic halide perovskites have recently emerged as promising candidates for low cost, high-efficiency solar cells. In this work, the electronic and optical properties of the triclinic lead-free hybrid halide perovskite $\text{CH}_3\text{NH}_3\text{SnI}_3$ as a solar cell absorber has been investigated using density functional theory and many body perturbation theory calculations. Depending on the functional used, Our calculated band gaps are 0.82, 1.25 and 1.32 eV, which agree well with the experimental result (1.21 and 1.35) eV [1]. In addition, our calculations show that that $\text{CH}_3\text{NH}_3\text{SnI}_3$ is a direct band gap semiconductor. Many body perturbation theory at the G_0W_0 level of approximation gives a fundamental band gap of 1.54 eV. In order to obtain optical spectra, we carried out Bethe-Salpeter equation calculations on top of non-self-consistent G_0W_0 calculations. Our calculated optical band gap shows anisotropy with an absorption edge of 1.22 eV for out-of-plane polarisation and 1.25 eV for in-plane polarisation. These values lie within the experimentally reported range, confirming that $\text{CH}_3\text{NH}_3\text{SnI}_3$ has potential as a solar cell absorber.

1. Introduction

Hybrid halide perovskites have recently emerged as potential new materials for solar cell applications leading to a new class of hybrid semiconductor photovoltaic cells [2, 3]. It is exemplified by the remarkable increase in power conversion efficiency from 3.8% by Miyasaka [4] to over 20% by Korea Research Institute of Chemical Technology (KRICT) [5] using low cost production methods. This performance is due to the exceptional properties of hybrid halide perovskites displaying high absorption coefficients, high carrier mobility, direct and tunable band gaps [6] and long charge carrier diffusion lengths [7, 8, 9]. Progress in efficiency, however, is hindered by many challenges such as the instability of many perovskite phases [10] and the toxicity of Pb in lead halide perovskites, the absorber in the prototypical high efficiency perovskite based solar cells [11]. Therefore, it is necessary to find an alternative material that does not contain toxic lead. A possible candidate is tin organic-inorganic halide perovskite,

$\text{CH}_3\text{NH}_3\text{SnX}_3$ ($X = \text{Cl}, \text{Br}$ or I), which has been reported to have a band gap of 1.21 eV and 1.35 eV depending on the preparation method [1]. Depending on temperature, $\text{CH}_3\text{NH}_3\text{SnX}_3$ ($X = \text{Cl}, \text{Br}$ or I) reveals a very rich phase diagram; i.e., the crystal structure of tin halide perovskite goes from cubic, tetragonal, orthorhombic and monoclinic to triclinic phase by cooling [12].

The first lead-free solar cell made of tin halide perovskite was demonstrated by the Noel et al. group [11] and the Hao et al. group [13] in 2014. Hao et al. investigated the photovoltaic properties of the tetragonal phase of $\text{CH}_3\text{NH}_3\text{SnI}_3$ and found that it has a direct-gap with an energy gap of 1.3 eV, which is significantly redshifted compared with $\text{CH}_3\text{NH}_3\text{PbI}_3$, whose band gap is 1.55 eV [14, 15]. Theoretical studies were carried out by Paolo Umari et al. [16] using GW calculations including spin orbit coupling of $\text{CH}_3\text{NH}_3\text{XI}_3$ ($X = \text{Pb}, \text{Sn}$) in the tetragonal phase. Their calculations gave band gaps of 1.67 eV and 1.10 eV for $\text{CH}_3\text{NH}_3\text{PbI}_3$ and $\text{CH}_3\text{NH}_3\text{SnI}_3$ respectively. They showed $\text{CH}_3\text{NH}_3\text{SnI}_3$ to be a better candidate for electron transport than $\text{CH}_3\text{NH}_3\text{PbI}_3$.

In this work, we perform density functional theory (DFT) calculations of the electronic and optical properties focusing on the triclinic phase of the $\text{CH}_3\text{NH}_3\text{SnI}_3$. To the best of our knowledge, the electronic and optical properties of the triclinic phase of $\text{CH}_3\text{NH}_3\text{SnI}_3$ have not been investigated extensively. We hope that the present investigation will contribute to a better theoretical understanding of the properties of this material, especially its potential in low band gap solar cell applications.

2. Methodology

The crystal structure of the triclinic phase of the hybrid halide perovskite ($\text{CH}_3\text{NH}_3\text{SnI}_3$) is shown in Figure 1. The unit cell of $\text{CH}_3\text{NH}_3\text{SnI}_3$ contains 24 H atoms, 4 Pb atoms, 4 C atoms, 12 I atoms, and 4 N atoms. With $a = 9.06 \text{ \AA}$, $b = 9.06 \text{ \AA}$ and $c = 12.56 \text{ \AA}$ (Material Project ID: mp-995238). In this work, the investigation of the electronic structure properties was performed

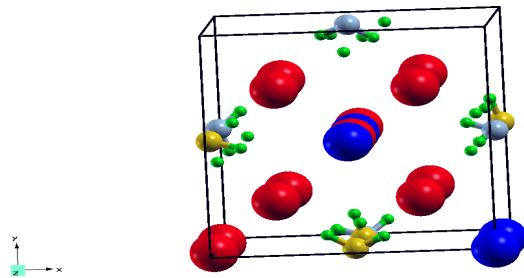


Figure 1. (Color online) The crystal structure of the triclinic phase of $\text{CH}_3\text{NH}_3\text{SnI}_3$ (green: hydrogen; grey: nitrogen; yellow: carbon; red: iodine; blue: tin).

using the Vienna Ab-initio Simulation Package (VASP) [17, 18] based on Density Functional Theory (DFT) [19, 20]. The Projector-Augmented Wave (PAW) [21] method was employed to treat the electron-ion interactions. To describe the electrons exchange and correlation effects, we used the Generalized Gradient Approximation (GGA) as parametrized by Perdew, Burke and Ernzerhof (PBE) [22], the modified Becke-Johnson (MBJ) [23] and the hybrid functional HSE06 [24], where the Hartree-Fock screening parameter μ is set at 0.2 \AA^{-1} . $4 \times 4 \times 4$ Monkhorst-Pack meshes were used in sampling the Brillouin zone (BZ) with an energy cut-off of 520 eV. These parameters were found to be sufficient for energy convergence. The BZ sampling was chosen in such a way that the convergence of free energy is less than 1 meV/atom. The convergence

threshold for self-consistent field iteration was set at 10^{-6} eV.

In order to study the optical properties, we performed non-selfconsistent G_0W_0 [25] calculations with 4008 bands and with an energy plane wave cut-off of 300 eV and a cut-off of 150 eV for the plane wave basis of the response function expansion. Optical spectra were calculated at the BSE [26] level of approximation with input from a G_0W_0 calculations.

3. Results and Discussions

3.1. Electronic Properties

The Kohn-Sham band structure of the studied material was calculated using the PBE functional. The calculated electronic band structure and its corresponding total and partial density of states (TDOS and PDOS) are displayed in Figure 2. The electronic band structure calculations demonstrate that this phase has a DFT direct band gap at the gamma point. We note from the PDOS that the valence band edge is dominated by I orbitals and the conduction band edge by Sn orbitals. The organic cation CH_3NH_3^+ do not have any significant contribution around the band edge. Our calculated approximate DFT and many body perturbation theory GW fundamental band gaps for the triclinic perovskite $\text{CH}_3\text{NH}_3\text{SnI}_3$ are listed in Table 1. The only available experimental data is that reported by Stoumpos et al. [1], where, depending on the preparation method, they reported that the experimental band gap of tin based hybrid halide perovskites to be 1.21 eV and 1.35 eV. Our results are consistent with these results.

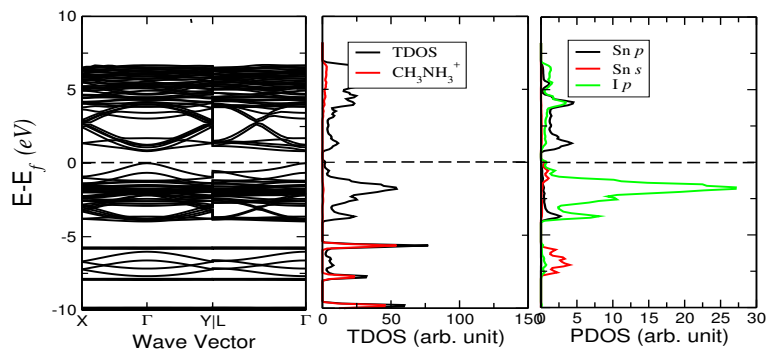


Figure 2. DFT calculated electronic structure of the triclinic phase of $\text{CH}_3\text{NH}_3\text{SnI}_3$ using PBE: band structure (left), total density of states (TDOS) and the partial density of states (PDOS) due to CH_3NH_3^+ (middle); and PDOS due to Sn and I (right).

Table 1. Our calculated and the experimental band gap of triclinic $\text{CH}_3\text{NH}_3\text{SnI}_3$.

Functional	PBE	MBJ	HSE06	GW	Exp.[1]
Band gap (eV)	0.82	1.25	1.32	1.54	1.21 and 1.35

3.2. Optical Properties

The optical properties can be calculated from the complex dielectric tensor, $\varepsilon(\omega) = \varepsilon_1(\omega) + i\varepsilon_2(\omega)$ which describes the polarization response of a material to an externally applied electric field \mathbf{E} . Using the real part $\varepsilon_1(\omega)$ and the imaginary part $\varepsilon_2(\omega)$ of the dielectric tensor $\varepsilon(\omega)$, we compute the optical absorption coefficient spectra. The results in Figure 3 show that the highest

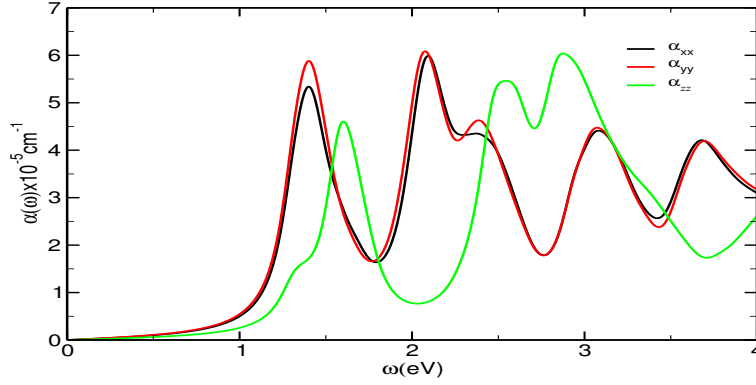


Figure 3. The optical absorption coefficient spectra of triclinic $\text{CH}_3\text{NH}_3\text{SnI}_3$.

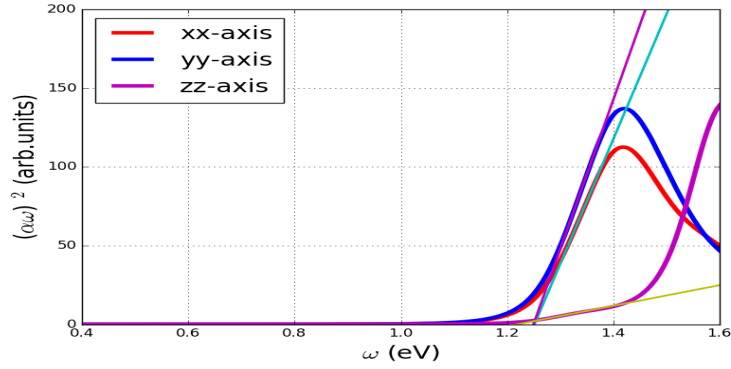


Figure 4. Tauc plot of the absorption coefficient, showing the polarization-dependent onsets.

absorption peak in the region (1.0-2.5) eV of $\alpha_{yy}(\omega)$ component is higher than that of $\alpha_{xx}(\omega)$ and $\alpha_{zz}(\omega)$. Figure 4 shows the absorption coefficient $\alpha(\omega)$ for triclinic $\text{CH}_3\text{NH}_3\text{SnI}_3$ plotted in Tauc formalism. From Figure 4 we can see there are featured edges as a function of polarization. Due to the structural anisotropy we observed variation of band edge in the different polarization. For in plane polarisation the onset is at 1.25 eV and for out of plane polarisation the onset is at 1.22 eV within the experimentally reported values (1.21 and 1.35) eV.

4. Conclusions

The electronic and optical properties of the triclinic $\text{CH}_3\text{NH}_3\text{SnI}_3$ have been calculated using first-principles methods. The material was found to be a direct band gap semiconductor. Depending on the method used, our calculated band gaps are 0.82 eV (PBE), 1.25 eV (MBJ), 1.32 eV (HSE06) and 1.54 eV (G_0W_0). Obtained values agree well with the experimental results (1.21 eV and 1.35 eV). Moreover, the BSE absorption edges using the Tauc form are found to be 1.22 eV for out-of-plane polarisation and 1.25 eV for in-plane polarisation. This anisotropy seen in the BSE absorption edges may be related to the experimental result 1.21 and 1.35 eV. Inspection of the obtained band structure, PDOS and TDOS reveals that the organic cation CH_3NH_3^+ does not have significant contribution around the band edges as I and Sn. Our results confirm that the triclinic phase of $\text{CH}_3\text{NH}_3\text{SnI}_3$ has potential as a solar cell absorber. Finally, with the help of the real part $\epsilon_{\text{re}}(\omega)$ and the imaginary part $\epsilon_{\text{im}}(\omega)$ of the dielectric tensor $\epsilon(\omega)$ we derive all the desired frequency dependent optical spectra such as absorption coefficient at

BSE level of approximation, which show a significant optical anisotropy.

5. Acknowledgement

IOAA would like to acknowledge the support he received from NRF-TWAS for funding, and Sudan University of Science and Technology (SUST). We also wish to acknowledge the Centre for High Performance Computing (CHPC), South Africa, for providing us with computing facilities.

References

- [1] Stoumpos C C, Malliakas C D and Kanatzidis M G 2013 *Inorganic Chemistry* **52** 9019–9038
- [2] Green M A and Ho-Baillie A 2017 *ACS Energy Letters* **2** 822–830
- [3] Park N G 2013 *The Journal of Physical Chemistry Letters* **4** 2423–2429
- [4] Kojima A, Teshima K, Shirai Y and Miyasaka T 2009 *Journal of the American Chemical Society* **131** 6050–6051
- [5] Yang W S, Noh J H, Jeon N J, Kim Y C, Ryu S, Seo J and Seok S I 2015 *Science* **348** 1234–1237
- [6] Noh J H, Im S H, Heo J H, Mandal T N and Seok S I 2013 *Nano Letters* **13** 1764–1769
- [7] Stranks S D, Eperon G E, Grancini G, Menelaou C, Alcocer M J, Leijtens T, Herz L M, Petrozza A and Snaith H J 2013 *Science* **342** 341–344
- [8] Dong Q, Fang Y, Shao Y, Mulligan P, Qiu J, Cao L and Huang J 2015 *Science* **347** 967–970
- [9] Shi D, Adinolfi V, Comin R, Yuan M, Alarousu E, Buin A, Chen Y, Hoogland S, Rothenberger A, Katsiev K *et al.* 2015 *Science* **347** 519–522
- [10] Zhang Y Y, Chen S, Xu P, Xiang H, Gong X G, Walsh A and Wei S H 2018 *Chinese Physics Letters* **35** 036104
- [11] Noel N K, Stranks S D, Abate A, Wehrenfennig C, Guarnera S, Haghighirad A A, Sadhanala A, Eperon G E, Pathak S K, Johnston M B *et al.* 2014 *Energy & Environmental Science* **7** 3061–3068
- [12] Feng J and Xiao B 2014 *The Journal of Physical Chemistry C* **118** 19655–19660
- [13] Hao F, Stoumpos C C, Cao D H, Chang R P and Kanatzidis M G 2014 *Nature Photonics* **8** 489
- [14] Eperon G E, Stranks S D, Menelaou C, Johnston M B, Herz L M and Snaith H J 2014 *Energy & Environmental Science* **7** 982–988
- [15] Ali I O A, Joubert D P and Suleiman M S H 2018 *Materials Today: Proceedings* **5** 10570–10576
- [16] Umari P, Mosconi E and De Angelis F 2014 *Scientific Reports* **4** 4467
- [17] Kresse G and Hafner J 1993 *Physical Review B* **47** 558
- [18] Kresse G and Hafner J 1994 *Physical Review B* **49** 14251
- [19] Hohenberg P and Kohn W 1964 *Physical Review* **136** B864
- [20] Kohn W and Sham L J 1965 *Physical Review* **140** A1133
- [21] Kresse G and Joubert D 1999 *Physical Review B* **59** 1758
- [22] Perdew J P, Burke K and Ernzerhof M 1996 *Physical Review Letters* **77** 3865
- [23] Becke A D and Johnson E R 2006 *The Journal of Chemical Physics* **124** 221101
- [24] Krukau A V, Vydrov O A, Izmaylov A F and Scuseria G E 2006 *The Journal of Chemical Physics* **125** 224106
- [25] Hedin L 1965 *Physical Review* **139** A796
- [26] Salpeter E E and Bethe H A 1951 *Physical Review* **84** 1232